

Multi-Robot Active Graph Exploration with Reduced Pose-SLAM Uncertainty via Submodular Optimization

Ruofei Bai^{1,2}, Shenghai Yuan¹, Hongliang Guo², Pengyu Yin¹, Wei-Yun Yau² and Lihua Xie¹, *Fellow, IEEE*

Abstract—This paper considers the multi-robot active graph exploration problem, where robots need to collaboratively cover a graph environment while maintaining reliable pose estimation in collaborative Simultaneous Localization and Mapping (SLAM). Considering both objectives presents challenges for multi-robot pathfinding, as it involves the expensive covariance propagation for SLAM uncertainty evaluation, especially when considering various combinations of robots’ paths. To reduce the computational complexity, we propose an efficient two-stage strategy where exploration paths are first generated for quick coverage, and then enhanced by adding informative loop-closing actions along the paths for reliable pose estimation. We formulate the latter problem as a non-monotone submodular maximization problem by relating SLAM uncertainty with pose graph topology, which (1) facilitates a more efficient evaluation of SLAM uncertainty than covariance inference, and (2) allows the employment of approximation algorithms in submodular optimization to provide suboptimality guarantees. We further introduce ordering heuristics to improve the objective values while preserving the optimality bound. Simulation experiments over randomly generated graph environments verify the effectiveness of our methods to achieve quick coverage and enhanced pose graph reliability, and benchmark the performance of the approximation algorithms and the greedy-based algorithm in the loop edge selection problem. Our implementations will be open-source at <https://github.com/bairuofei/CGE>.

I. INTRODUCTION

Multi-robot exploration holds immense promise in applications such as search and rescue [1], surveillance and inspection [2], [3], autonomous mapping [4], etc. However, challenges arise in GPS-denied environments like indoor, urban canyons, and tunnels, where robots need to estimate their pose with onboard sensors during exploration [5], [6]. Leveraging Multi-Robot SLAM [7] for Exploration (MRSE) allows for enhanced spatial awareness, with superior efficiency and robustness than using a single robot. Specifically, in pose graph-based multi-robot SLAM methods [8], robots incrementally construct individual pose graphs during exploration, which are connected by inter-robot loop closures. By aggregating pose graphs from robots in a central server, collaborative pose estimation can be achieved by multi-robot

*This research is supported by the National Research Foundation, Singapore under its Medium Sized Center for Advanced Robotics Technology Innovation; and in part by grant no. C221518004 from the Robotics HTC, Agency for Science, Technology and Research (A*STAR), Singapore.

¹Ruofei Bai, Shenghai Yuan, Pengyu Yin and Lihua Xie are with the School of Electrical and Electronic Engineering, Nanyang Technological University, Singapore 639798 {ruofei001, shyuan, pengyu001, elhxie}@ntu.edu.sg

²Ruofei Bai, Hongliang Guo and Wei-Yun Yau are with the Institute for Infocomm Research (I2R), Agency for Science, Technology and Research (A*STAR), Singapore 138632 {stubair, guo_hongliang, wyau}@i2r.a-star.edu.sg

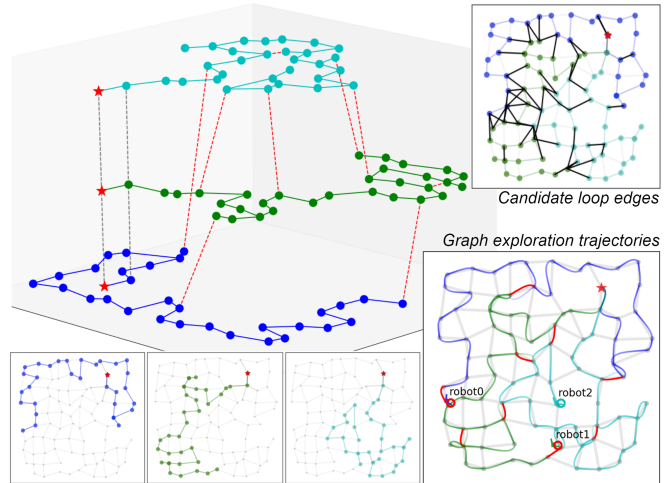


Fig. 1. The active graph exploration with three robots in a $100m \times 100m$ 2D graph environment (light gray). The robots’ exploration paths are colored in blue, green, and cyan, respectively, with the starting positions marked with red stars. The selected loop edges are colored in red, and the valid candidate loop edges are colored in black. The resulting exploration trajectories efficiently cover the whole graph, while forming a well-connected multi-robot pose graph topology to reduce SLAM uncertainty with informative and distance-efficient loop edges (colored in red).

pose graph optimization, mitigating single-robot odometry drift and ensuring consistent pose estimation among robots.

However, most existing works treat multi-robot SLAM and exploration as distinct problems [9], [10], and fail to find paths that can form well-connected pose graphs, which are implicitly required by existing SLAM methods to achieve reliable pose estimation [11]. Ignoring the pose graph reliability in MRSE problems may cause inconsistent pose estimations among robots due to weak connections in their individual pose graphs [12]. One feasible solution is to manually define robots’ trajectories to facilitate inter-robot loop closures. However, this limits the autonomy and efficiency of robots.

The challenges of MRSE include the high computational complexity in the planning stage to consider both exploration efficiency and pose graph reliability; and the lack of efficient metrics to evaluate the reliability of the multi-robot pose graph resulting from various combinations of robots’ candidate paths, which requires expensive covariance propagation [13], making it challenging for efficient planning.

In this paper, we address the above challenges by formulating them into a collaborative active graph exploration problem (see Fig. 1), where the robots need to find paths to cover a graph while maintaining a well-connected multi-robot pose graph for reliable pose estimation. To reduce the

computational complexity, we propose a two-stage strategy to solve the pathfinding problem, where exploration paths are first generated for quick coverage, and then enhanced by identifying and selecting informative loop-closing actions, called *loop edges*, along the generated paths. Based on the relationship between SLAM uncertainty and pose graph topology, the loop edge selection problem is formulated as a set optimization problem with a non-monotone submodular objective function, which avoids expensive covariance inference. Furthermore, it allows the employment of approximation algorithms in submodular optimization to provide optimality guarantees. The contributions of this paper are:

- An efficient two-stage strategy to the multi-robot graph exploration problem, which prioritizes both exploration efficiency and the reliability of collaborative pose estimation in multi-robot SLAM.
- A novel formulation of the informative and distance-efficient loop edge selection problem as a non-monotone submodular maximization problem, alongside the employment of existing approximation algorithms with optimality guarantees.

We conducted simulation experiments to demonstrate the effectiveness of the proposed methods to achieve quick coverage and reliable pose graph estimation, and benchmark the performance and time complexity of approximation algorithms and the greedy-based algorithm.

II. RELATED WORKS

A. Multi-Robot Active Exploration

Multi-robot active exploration aims to find an action sequence for a group of robots to actively explore the environment, considering several factors like energy consumption, target uncertainty reduction, etc. Existing methods in multi-robot active exploration can be generally classified into two types: search-based [14] and sampling-based [15]. They all aim to efficiently search an action space that increases exponentially w.r.t. the number of robots and the planning horizon. Previous work [14] considers multi-robot active exploration to estimate the distribution of targets in the environment, and applies the coordinate descent algorithm to provide $\frac{1}{2}$ optimality guarantee for the final selected paths. Cai *et al.* further considers energy-aware information gathering problem for multiple robots [16], where the robots' trajectories are selected by optimizing a non-monotone submodular function subject to partition matroid constraints. However, the trajectories of robots are evaluated separately, hence cooperative sensing among robots is not considered.

The aforementioned works require covariance propagation to evaluate the effect of future actions, which is computationally expensive. To alleviate this issue, recent works have used topology metrics to approximate the covariance inference in active SLAM [17], [18], and belief space planning [10], which brings significantly lower computational complexity. Specifically, Khosoussi *et al.* show that the Fisher Information Matrix (FIM) in the pose graph optimization problem is related to the pose graph Laplacian matrix weighted by the

corresponding covariance matrices [19]. Chen *et al.* further extend this work into 3D case [20]. Additionally, Placed *et al.* directly encapsulate the covariance matrix of each measurement as the edge weight of the Laplacian matrix, providing an efficient approximation of the FIM [21].

This paper also uses the topology metrics for pose-SLAM uncertainty evaluation like in [19], [10], but further considers balancing the distance cost in a graph exploration task, which results in a non-monotone objective function. Moreover, by utilizing a graph representation of the environment, this paper finds multiple loop edges in robots' pathfinding to form a globally reliable pose graph, while related works [17], [18] adopt reactive strategies that only need to find the single best loop edge within a local horizon. This paper extends our previous work [22] about single-robot SLAM-aware path planning to the multi-robot case. Previous work provides no performance guarantees by using a simple greedy algorithm with pruning techniques for loop edge selection. Instead, by reformulating the objective function in this paper, approximation algorithms for submodular maximization can be used to find solutions with optimality guarantees.

III. PRELIMINARIES

A. Submodular and Monotone Set Function

Let $f : 2^{\mathcal{N}} \rightarrow \mathbb{R}$ be a set function defined on a ground set \mathcal{N} consisting of finite elements. For a set $A \subseteq \mathcal{N}$ and $u \in \mathcal{N}$, we define $\Delta_f(u|A) = f(A \cup \{u\}) - f(A)$ for a given set function $f(\cdot)$ as its marginal profit when adding an element u to an existing set A .

Definition 1 (Submodularity): A set function $f : 2^{\mathcal{N}} \rightarrow \mathbb{R}$ is submodular if $\Delta_f(u|A) \geq \Delta_f(u|B), \forall A \subseteq B \subseteq \mathcal{N}, u \in \mathcal{N} \setminus B$.

Definition 2 (Monotonicity): A set function $f : 2^{\mathcal{N}} \rightarrow \mathbb{R}$ is monotone if for any $A \subseteq B \subseteq \mathcal{N}$, $f(A) \leq f(B)$.

B. Graph Laplacian Matrix

Given a connected graph \mathcal{G} with $n + 1$ vertices and m edges, the graph Laplacian matrix is defined as:

$$\mathbf{L}^\circ = \mathbf{B}^\circ \mathbf{B}^{\circ\top} = \sum_{k=1}^m \mathbf{B}_k \mathbf{B}_k^\top \in \mathbb{R}^{(n+1) \times (n+1)}, \quad (1)$$

where $\mathbf{B}^\circ \in \mathbb{R}^{(n+1) \times m}$ is the incidence matrix, \mathbf{B}_k is the k -th column vector of \mathbf{B}° that only has non-zero values at two indices corresponding to the vertices connected by the k -th edge. The weighted Laplacian matrix of the graph \mathcal{G} is defined as $\mathbf{L}_\gamma^\circ = \mathbf{B}^\circ \text{Diag}\{\gamma_1, \dots, \gamma_m\} \mathbf{B}^{\circ\top}$, where γ_k is the weight of k -th edge in \mathcal{G} . If one vertex is anchored in \mathcal{G} , *i.e.*, the corresponding row is removed from the incidence matrix \mathbf{B}° , the obtained Laplacian matrix is called the reduced Laplacian matrix, denoted as $\mathbf{L} \in \mathbb{R}^{n \times n}$. The reduced weighted Laplacian matrix \mathbf{L}_γ can be defined similarly.

C. Collaborative Multi-Robot Pose Graph Optimization

In a multi-robot pose-SLAM system with a set of robots $\mathcal{R} = \{1, 2, \dots, R\}$, each robot $r \in \mathcal{R}$ incrementally constructs an individual pose graph $\mathcal{G}_r^{\text{pose}} = \langle \mathcal{X}_r, \mathcal{Z}_r \rangle$ for pose estimation, where \mathcal{X}_r is a set of poses that correspond to the selected keyframes from sensor readings, *e.g.*, lidar

scans or camera frames, and $\forall x_i \in \mathcal{X}_r$, $x_i \in \text{SE}(2)$ or $\text{SE}(3)$; $\mathcal{Z}_r = \{\langle x_i, x_j \rangle | x_i, x_j \in \mathcal{X}_r\}$ contains relative observations between pairs of poses in $\mathcal{G}_r^{\text{pose}}$, established by either odometry estimation or loop closure detection [8]. By sharing individual pose graphs with a central server, a collaborative multi-robot pose graph $\mathcal{G}_{\mathcal{R}}^{\text{pose}} = \langle \mathcal{X}, \mathcal{Z} \rangle$ can be constructed by connecting all individual pose graphs with inter-robot loop closures, where $\mathcal{X} = \cup_{r \in \mathcal{R}} \mathcal{X}_r$ and $\mathcal{Z} = (\cup_{r \in \mathcal{R}} \mathcal{Z}_r) \cup \mathcal{Z}^{\text{inter}}$. The set $\mathcal{Z}^{\text{inter}}$ includes all inter-robot observations among robots. Each $z_{ij} \in \mathcal{Z}$ is assumed to follow a Gaussian distribution $\mathcal{N}(\hat{z}_{ij}(x_i, x_j), \Sigma_{ij})$, where $\hat{z}_{ij}(x_i, x_j)$ represents the expected transformation between x_i and x_j , Σ_{ij} is the covariance matrix for the actual observation z_{ij} . Given all relative observations \mathcal{Z} , the multi-robot pose graph optimization aims to find the best estimation of robots' poses \mathcal{X} , which is equivalent to the following nonlinear least square problem [7]:

$$\min_{\mathcal{X}} \mathbf{F}(\mathcal{X}) = \sum_{z_{ij} \in \mathcal{Z}} e_{ij}^{\top} \Sigma_{ij}^{-1} e_{ij}, \quad (2)$$

where $e_{ij} = z_{ij} - \hat{z}_{ij}(x_i, x_j)$. A local optimal estimation of \mathcal{X} can be found using iterative local search methods, like the Gauss-Newton method or Levenberg–Marquardt algorithm.

The Hessian matrix \mathbf{H} of the pose graph optimization problem is derived as:

$$\mathbf{H} = \frac{1}{2} \sum_{z_{ij} \in \mathcal{Z}} \mathbf{J}_{ij}^{\top} \Sigma_{ij}^{-1} \mathbf{J}_{ij} = \frac{1}{2} \sum_{z_{ij} \in \mathcal{Z}} \mathbf{B}_{ij} \mathbf{B}_{ij}^{\top} \otimes \tilde{\Sigma}_{ij}^{-1}, \quad (3)$$

where \mathbf{J}_{ij} is the Jacobi matrix of the residual term e_{ij} w.r.t. a vector of all variables in \mathcal{X} , $\mathbf{B}_{ij} \mathbf{B}_{ij}^{\top}$ is the Laplacian factor corresponding to the edge z_{ij} in $\mathcal{G}_{\mathcal{R}}^{\text{pose}}$; $\tilde{\Sigma}_{ij}$ is derived from the transformation of Σ_{ij} . The detailed derivation of Eq. (3) is referred to [21].

D. Relating Pose Graph Uncertainty with Graph Topology

In practice, the Hessian matrix \mathbf{H} is also known as the *observed FIM* [23], denoted as $\mathbb{I}(\mathbf{x})$. It provides a lower bound approximation of the covariance matrix in pose graph optimization according to the Cramér–Rao bound. Scalar functions for \mathbf{H} or $\mathbb{I}(\mathbf{x})$ can therefore be used to quantify the pose-SLAM uncertainty, among which the D-optimal is shown to be superior in capturing the global uncertainty in all dimensions of the poses [24]. The D-optimal is a scalar function from Theory of Optimal Experimental Design [25] and is defined as $D\text{-opt}(\mathbf{L}) = \det(\mathbf{L})^{\frac{1}{n}}$ for an $n \times n$ matrix.

According to [21], the D-optimal of the FIM $\mathbb{I}(\mathbf{x})$ in pose graph optimization can be well-approximated by the D-optimal of the reduced Laplacian matrix of the pose graph with proper edge weights:

$$\begin{aligned} D\text{-opt}(\mathbb{I}(\mathbf{x})) &= D\text{-opt}\left(\sum_{z_{ij} \in \mathcal{Z}} \mathbf{B}_{ij} \mathbf{B}_{ij}^{\top} \otimes \tilde{\Sigma}_{ij}^{-1}\right) \\ &\approx D\text{-opt}\left(\sum_{z_{ij} \in \mathcal{Z}} \mathbf{B}_{ij} \mathbf{B}_{ij}^{\top} \cdot D\text{-opt}(\tilde{\Sigma}_{ij}^{-1})\right) = D\text{-opt}(\mathbf{L}_{\gamma}). \end{aligned} \quad (4)$$

The subscript γ in \mathbf{L}_{γ} indicates that each edge z_{ij} in the pose graph is weighted by $D\text{-opt}(\tilde{\Sigma}_{ij}^{-1})$. Note that Eq. (4) establishes the relationship between the pose graph reliability and graph topology, which is used in this paper for pose graph uncertainty evaluation. It brings two main advantages:

- (1) the impact of adding loop closures to a pose graph can be directly evaluated through the graph Laplacian matrix without multi-robot covariance inference;
- (2) the dimension of the weighted graph Laplacian only depends on the number of poses in the pose graph, regardless of the pose dimension, which is computationally more efficient.

IV. PROBLEM STATEMENT

This paper considers the problem where a set of robots $\mathcal{R} = \{1, \dots, R\}$ are required to explore an environment represented as a graph $\mathcal{G} = \langle \mathcal{V}, \mathcal{E}, \omega \rangle$, as shown in Fig. 1, where $\mathcal{V} \subseteq \mathbb{R}^2/\mathbb{R}^3$ is a set of places of interests distributed in a 2D (or 3D) environment; $\mathcal{E} \subseteq \mathcal{V} \times \mathcal{V}$ includes pairs of vertices that are directly connected; $\omega : \mathcal{E} \rightarrow \mathbb{R}_{\geq 0}$ is the distance function for the edges. The graph \mathcal{G} is a discretized representation of an environment, which can be obtained from a prior topological map [26], an existing roadmap, or derived from the Voronoi partition of the environment [27]. The robots are initially distributed over the vertices of \mathcal{G} , denoted as the set $\{v_r^0\}_{r \in \mathcal{R}}$. The problem is to find a set of paths $\{\mathcal{P}_r\}_{r \in \mathcal{R}}$ starting from $\{v_r^0\}_{r \in \mathcal{R}}$, following which the robots in \mathcal{R} can (1) quickly cover all vertices in \mathcal{G} ; (2) maintain reliable multi-robot pose graph topology to reduce SLAM uncertainty.

A. The Two-Stage Strategy

The above problem directly relates to the Vehicle Routing Problem (VRP), *i.e.*, a generalization of the Traveling Salesman Problem to multiple robots, and is generally NP-Hard [28]. It requires finding paths for several robots to visit specified locations once in the environment starting and ending at a depot, while minimizing the maximum single robot's distance. To reduce the planning complexity and facilitate existing VRP solvers, we divide the original problem into two stages, as shown in Fig. 2.

- Stage 1: VRP pathfinding. The first stage solves a standard VRP problem over the graph \mathcal{G} to find the shortest paths for robots for quick graph coverage. Existing VRP solvers like OR-Tools [29] can be used to provide sub-optimal solutions to the problem.
- Stage 2: Loop edge selection. Given the VRP paths, Stage 2 opportunistically finds informative and distance-efficient loop-closing actions to be inserted into the paths to form a reliable multi-robot pose graph topology.

The two-stage strategy sequentially considers both exploration efficiency and pose graph reliability, avoiding intractable search that considers all possible combinations of robots' paths. Specifically, in Stage 1, the VRP problem is defined over \mathcal{G} . The starting vertices of robots are defined as their initial located vertices $\{v_r^0\}_{r \in \mathcal{R}}$, while the ending vertices are not specified to encourage quick coverage. The obtained VRP path for robot $r \in \mathcal{R}$ is denoted as $\mathcal{P}_r^{\text{VRP}}$, which is a list of vertices in \mathcal{G} . The robots can follow the VRP paths $\{\mathcal{P}_r^{\text{VRP}}\}_{r \in \mathcal{R}}$ to achieve quick coverage of \mathcal{G} . Then in Stage 2, we focus on finding informative loop edges to enhance the VRP paths, as introduced in the following subsections.

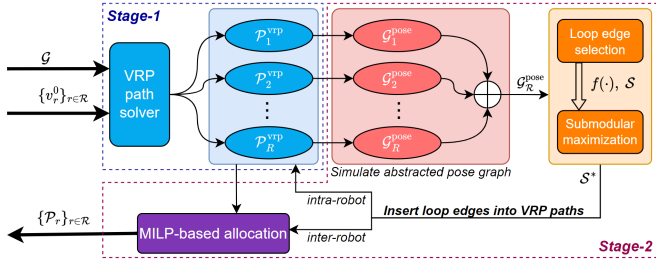


Fig. 2. The framework of the proposed method, which takes inputs of a graph representation of the environment \mathcal{G} and robots' initial positions $\{v_r^0\}_{r \in \mathcal{R}}$, and finally outputs the robots' paths $\{P_r\}_{r \in \mathcal{R}}$ that can cover the environment while resulting in a well-connected multi-robot pose graph.

B. Hierarchical Abstraction of Multi-Robot Pose Graph

This section describes how to approximate an *abstracted* multi-robot pose graph, as the robots follow their VRP paths to explore the graph \mathcal{G} . The abstracted pose graph is used to identify informative loop-closing actions during multi-robot exploration for reliable SLAM estimation. Specifically, by following P_r^{vrp} , robot r covers a subgraph of \mathcal{G} , which can be treated as a *hierarchical abstraction* of the robot r 's SLAM pose graph. In this paper, we directly use such abstracted pose graph for SLAM uncertainty evaluation, motivated by the hierarchical pose graph optimization [30]. As introduced in [22], the abstracted pose graph is defined as follows.

Definition 3 (abstracted pose graph): Given a path P_r^{vrp} over a graph $\mathcal{G} = \langle \mathcal{V}, \mathcal{E}, \omega \rangle$, an abstracted pose graph corresponding to P_r^{vrp} is defined as $\mathcal{G}_r^{\text{pose}} = \langle \mathcal{X}_r, \mathcal{Z}_r \rangle$, where each pose $x_i \in \mathcal{X}_r$ corresponds uniquely to a vertex visited by P_r^{vrp} , and an edge $z_{ij} = \langle x_i, x_j \rangle \in \mathcal{Z}_r$ exists iff the corresponding vertices of the two poses x_i and x_j are visited consecutively in P_r^{vrp} .

Moreover, we define $\mathcal{M}_{\mathcal{X}} : \mathcal{X} \rightarrow \mathcal{V}$ as a mapping function from robot poses to vertices in \mathcal{G} , and $\mathcal{M}_{\mathcal{Z}} : \mathcal{Z} \rightarrow \mathcal{E}$ as a mapping function from edges in $\mathcal{G}_r^{\text{pose}}$ to those in \mathcal{G} . We have $\mathcal{M}_{\mathcal{X}}(\mathcal{X}_r) \subseteq \mathcal{V}$, $\mathcal{M}_{\mathcal{Z}}(\mathcal{Z}_r) \subseteq \mathcal{E}$; and $\cup_{r \in \mathcal{R}} \mathcal{M}_{\mathcal{X}}(\mathcal{X}_r) \equiv \mathcal{V}$ as the VRP paths guarantee that the graph \mathcal{G} is fully explored. With a slight notation abuse, we define the distance metric $\omega(z_{ij}) = \omega(\mathcal{M}_{\mathcal{Z}}(z_{ij}))$, for each edge $z_{ij} \in \mathcal{Z}_r$.

Remark 1: If the edge lengths in the original \mathcal{G} vary significantly, we can add additional vertices along the long edges in \mathcal{G} to make them balanced for better approximation of the abstracted pose graph. Meanwhile, the connectivity information in \mathcal{G} remains unchanged.

Remark 2: The orientation of poses in the abstracted pose graph is not properly defined in Def. 3, because $\mathcal{V} \subseteq \mathbb{R}^2/\mathbb{R}^3$ for vertices in \mathcal{G} and P_r^{vrp} , but $\mathcal{X}_r, \mathcal{Z}_r \subseteq \text{SE}(2)/\text{SE}(3)$. However, we claim that the absolute value of the orientation has no impact on evaluation of the pose graph uncertainty, as Eq. (4) only involves the observation uncertainty.

Additionally, we have the following assumption to capture the inter-robot loop closures formed by the VRP paths.

Assumption 1: If two robots visit the same vertex, an inter-robot loop closure is assumed to be established between the two corresponding poses in their pose graphs.

With assumption 1, an abstracted multi-robot pose graph

$\mathcal{G}_{\mathcal{R}}^{\text{pose}} = \langle \mathcal{X}, \mathcal{Z} \rangle$ can be constructed by connecting all abstracted pose graphs $\{\mathcal{G}_r^{\text{pose}}\}_{r \in \mathcal{R}}$ with inter-robot loop closures. We define the mapping function $\mathcal{M}_{\mathcal{R}} : \mathcal{X} \rightarrow \mathcal{R}$ that maps a pose $x_i \in \mathcal{X}$ to its corresponding robot. Note in the following text, we may omit the term "abstracted" when there is no ambiguity.

C. Loop Edge Selection over Abstracted Pose Graph

With the abstracted multi-robot pose graph $\mathcal{G}_{\mathcal{R}}^{\text{pose}}$, we can then identify *informative* and *distance-efficient* loop-closing actions, called loop edges, over $\mathcal{G}_{\mathcal{R}}^{\text{pose}}$ to reduce the pose estimation uncertainty in multi-robot SLAM. We define candidate loop edges in $\mathcal{G}_{\mathcal{R}}^{\text{pose}}$ as follows.

Definition 4 (Loop edge): A candidate loop edge connects two poses that are not directly connected in $\mathcal{G}_{\mathcal{R}}^{\text{pose}}$. Given $\mathcal{G}_{\mathcal{R}}^{\text{pose}} = \langle \mathcal{X}, \mathcal{Z} \rangle$, the set of all candidate loop edges is defined as $\mathcal{S} = \{\langle x_i, x_j \rangle \mid x_i, x_j \in \mathcal{X}; i < j; \langle x_i, x_j \rangle \notin \mathcal{Z}\}$, where $\langle x_i, x_j \rangle$ is also denoted as z_{ij} for simplicity.

The covariance matrix Σ_{ij} attached to loop edge z_{ij} is defined as a constant if no prior information about feature distribution is available, or can be set proportional to the number of features around $\mathcal{M}_{\mathcal{X}}(x_i)$ and $\mathcal{M}_{\mathcal{X}}(x_j)$ in the environment as in [31].

Remark 3: A loop edge $\langle x_i, x_j \rangle$ is not a loop closure, but a continuous action to establish loop closure between x_i and x_j , i.e., the robot $\mathcal{M}_{\mathcal{R}}(x_j)$ will move from $\mathcal{M}_{\mathcal{X}}(x_j)$ towards another vertex $\mathcal{M}_{\mathcal{X}}(x_i)$ in \mathcal{G} to establish loop closures. During this process, a chain of poses and edges may be added into $\mathcal{G}_{\mathcal{R}}^{\text{pose}}$ depending on the distance between $\mathcal{M}_{\mathcal{X}}(x_i)$ and $\mathcal{M}_{\mathcal{X}}(x_j)$, rather than only one loop closure. Previous work [17] has provided a bounded one-edge approximation of the chain structure based on Kirchhoff's matrix-tree theorem [32] to facilitate efficient evaluation of the graph topology metric. However, it leads to repeated approximation when approximating multiple chain structures, i.e., multiple loop edges, and thus loses the approximation bounds. To supplement that, here we further penalize long loop edges with their distance metrics to avoid distance-costly actions, while using one-edge approximation when evaluating their contribution to the SLAM uncertainty reduction.

After constructing a set \mathcal{S} of candidate loop edges, we define the loop edge selection problem as follows:

Problem 1: Given a multi-robot pose graph $\mathcal{G}_{\mathcal{R}}^{\text{pose}}$ and a ground set \mathcal{S} of candidate loop edges, find a subset $\mathcal{S}' \in 2^{\mathcal{S}}$ so that the following objective function is maximized:

$$f(\mathcal{S}') = \frac{1}{n} \log \det \left(\mathbf{L}(\mathcal{G}_{\mathcal{R}}^{\text{pose}}) + \sum_{z_{ij} \in \mathcal{S}'} \gamma_{ij} \mathbf{B}_{ij} \mathbf{B}_{ij}^{\top} \right) - \alpha \cdot \sum_{z_{ij} \in \mathcal{S}'} 2 \cdot \omega(z_{ij}) + d^{\max}, \quad (5)$$

where $f : 2^{\mathcal{S}} \rightarrow \mathbb{R}$ is a set function defined over the ground set \mathcal{S} ; $\mathbf{L}(\mathcal{G}_{\mathcal{R}}^{\text{pose}})$ is the reduced weighted Laplacian matrix corresponding to $\mathcal{G}_{\mathcal{R}}^{\text{pose}}$, with starting poses of robots anchored; α is a parameter that balances the graph topology metric and the distance metric; d^{\max} is a constant that keeps $f(\cdot)$ being positive, and is defined as $d^{\max} = 2 \cdot \max\{\omega(z_{ij}) \mid z_{ij} \in \mathcal{S}\} \cdot |\mathcal{S}|$.

In Problem 1, the first term $\frac{1}{n} \log \det(\mathbf{L}(\cdot))$ in $f(\cdot)$ quantifies the multi-robot SLAM uncertainty after adding a set \mathcal{S}' of loop edges into $\mathcal{G}_{\mathcal{R}}^{\text{pose}}$. It is a pose graph topology metric that directly relates to the FIM in pose graph optimization, as introduced in Sec. III-D. By selecting a loop edge z_{ij} , an edge connecting x_i and x_j is added to $\mathcal{G}_{\mathcal{R}}^{\text{pose}}$. Hence the Laplacian matrix is updated as $\mathbf{L}(\mathcal{G}_{\mathcal{R}}^{\text{pose}}) + \gamma_{ij} \mathbf{B}_{ij} \mathbf{B}_{ij}^{\top}$, where γ_{ij} is the encapsulated weight for the edge z_{ij} with covariance Σ_{ij} . Each selected loop edge z_{ij} introduces extra distance cost of $2 \cdot \omega(z_{ij})$, where the multiplier 2 comes from an assumption that a robot will follow the path $\langle x_j, x_i, x_j \rangle$ to establish loop closures with x_i and then go back to x_j to continue exploration.

The objective function $f(\cdot)$ in Problem 1 encourages the addition of loop edges into the robot's VRP paths, to improve the graph topology metric, thereby reduce the pose-SLAM uncertainty. Meanwhile, it also penalizes distance-costly loop edges to maintain quick coverage. Problem 1 is similar to the edge selection problem in [19], but further considers the distance cost, in which case a simple greedy algorithm as in [19] has no optimality guarantee. We will introduce the algorithms to solve Problem 1 in Sec. V.

D. Design of Parameter α in Problem 1

The parameter α in Eq. (5) relates to multiple factors, including the topology of the graph \mathcal{G} , the environmental area covered by \mathcal{G} , and the distribution of potential loop edges in $\mathcal{G}_{\mathcal{R}}^{\text{pose}}$, which presents challenges to provide a closed-form definition for α . Instead, we employ a more practical numerical approach to derive α in this work. Specifically, we define two bounds $\alpha^{\max} = \max_{z_{ij} \in \mathcal{S}} \frac{\Delta_f(z_{ij}|\emptyset)}{2 \cdot \omega(z_{ij})}$, $\alpha^{\min} = \min_{z_{ij} \in \mathcal{S}} \frac{\Delta_f(z_{ij}|\emptyset)}{2 \cdot \omega(z_{ij})}$, which corresponds to the two loop edges in \mathcal{S} that have the most and the least contributions to the objective function $f(\cdot)$. A reasonable α should be within the interval $[\alpha^{\min}, \alpha^{\max}]$ because: (1) if $\alpha > \alpha^{\max}$, no loop edge in \mathcal{S} can improve the objective value $f(\emptyset)$ because of the submodularity (proved in Sec. V-A); (2) if $\alpha < \alpha^{\min}$, all candidate loop edges in \mathcal{S} will be taken into consideration, even those connecting two poses that are far from each other and being distance-costly. Therefore, we define α as:

$$\alpha = \alpha^{\min} + \lambda(\alpha^{\max} - \alpha^{\min}), \quad (6)$$

where $\lambda \in (0, 1)$ controls how many candidate loop edges in \mathcal{S} is valid in Problem 1, e.g., a candidate loop edge z_{ij} with $\frac{\Delta_f(z_{ij}|\emptyset)}{2 \cdot \omega(z_{ij})} \leq \alpha$ will be discarded; and influences the number of finally selected loop edges in Problem 1.

E. MILP-based Loop Edge Allocation and Insertion

After solving Problem 1, a set of selected loop edges is obtained, denoted as \mathcal{S}^* . They are allocated to robots to balance their workload and inserted into their VRP paths. First, for each loop edge $z_{ij} \in \mathcal{S}^*$ that satisfies $\mathcal{M}_{\mathcal{R}}(x_i) = \mathcal{M}_{\mathcal{R}}(x_j)$, i.e., z_{ij} aims to establish intra-robot loop closure of robot $\mathcal{M}_{\mathcal{R}}(x_i)$, a sequence $\langle x_j, x_i, x_j \rangle$ is directly inserted into the corresponding position in the robot's VRP path. Second, for all z_{ij} that satisfies $\mathcal{M}_{\mathcal{R}}(x_i) \neq \mathcal{M}_{\mathcal{R}}(x_j)$, the loop

edge is allocated to either $\mathcal{M}_{\mathcal{R}}(x_i)$ or $\mathcal{M}_{\mathcal{R}}(x_j)$, depending on the results of balancing distance cost among robots. Specifically, all such loop edges are allocated to the related robots by solving a mixed integer linear program (MILP) that minimizes the maximum distance of each involved robot, and then inserted into their allocated robots' VRP paths as in the first case. The details are omitted here due to space limitations and refer to the attached video. The final paths for multi-robot graph exploration can then be obtained, denoted as $\{\mathcal{P}_r\}_{r \in \mathcal{R}}$.

V. METHODOLOGY

This section first proves the submodularity of the objective function in Problem 1, and then introduces approximation algorithms in submodular maximization to find sub-optimal solutions \mathcal{S}^* to Problem 1 with optimality guarantees.

A. Submodularity of Objective Function in Problem 1

Proposition 1: The set function $f(\cdot)$ in Problem 1 is a non-monotone submodular function.

Proof: According to the objective function (5), adding a loop edge will increase the graph connectivity metric but will also introduce additional distance cost. Therefore, the monotonicity of $f(\cdot)$ is not preserved. To prove submodularity, it is equivalent to prove $\Delta_f(z_{ij}|A) \geq \Delta_f(z_{ij}|B)$, $\forall z_{ij} \in \mathcal{S} \setminus B$ and $A \subseteq B \subseteq \mathcal{S}$. We have $\Delta_f(z_{ij}|A) = \frac{1}{n} \log \det(\mathbf{L}_A + \gamma_{ij} \mathbf{B}_{ij} \mathbf{B}_{ij}^{\top}) - \frac{1}{n} \log \det(\mathbf{L}_A) - \alpha \cdot \omega(z_{ij})$, where $\mathbf{L}_A = \mathbf{L}(\mathcal{G}_{\mathcal{R}}^{\text{pose}}) + \sum_{\langle x_i, x_j \rangle \in A} \gamma_{ij} \mathbf{B}_{ij} \mathbf{B}_{ij}^{\top}$ for notation simplicity. According to the matrix determinant lemma, it holds that:

$$\det(\mathbf{L}_A + \gamma_{ij} \mathbf{B}_{ij} \mathbf{B}_{ij}^{\top}) = \det(\mathbf{L}_A) \det(1 + \gamma_{ij} \mathbf{B}_{ij}^{\top} \mathbf{L}_A^{-1} \mathbf{B}_{ij}).$$

Thus we have

$$\Delta_f(z_{ij}|A) = \frac{1}{n} \log \det(1 + \gamma_{ij} \mathbf{B}_{ij}^{\top} \mathbf{L}_A^{-1} \mathbf{B}_{ij}) - \alpha \cdot \omega(z_{ij}).$$

Similarly, $\Delta_f(z_{ij}|B) = \frac{1}{n} \log \det(1 + \gamma_{ij} \mathbf{B}_{ij}^{\top} \mathbf{L}_B^{-1} \mathbf{B}_{ij}) - \alpha \cdot \omega(z_{ij})$. To prove $\Delta_f(z_{ij}|A) \geq \Delta_f(z_{ij}|B)$, it is sufficient to show that $\gamma_{ij} \mathbf{B}_{ij}^{\top} \mathbf{L}_A^{-1} \mathbf{B}_{ij} \geq \gamma_{ij} \mathbf{B}_{ij}^{\top} \mathbf{L}_B^{-1} \mathbf{B}_{ij}$, which has been proved similarly as in *Proof 1* of [22]. This concludes the proof of the submodularity of the function $f(\cdot)$. ■

B. Submodular Maximization with Ordering Heuristics

With Prop. 1, the Problem 1 is recognized as an unconstrained submodular maximization (USM) problem. Existing approximation algorithms in submodular optimization can be used to solve Problem 1 with optimality guarantees. In this paper, we employ two algorithms, i.e., *doubleGreedy* [33] and *deterministicUSM* [34] algorithms to solve the problem, both of which provide $\frac{1}{2}$ optimality guarantee¹. The two algorithms treat the objective function $f(\cdot)$ as an oracle function and query $f(\cdot)$ for objective values. The details of the two algorithms are referred to [33] and [34], respectively.

Furthermore, we introduce the ordering heuristics to the above two algorithms, as in Alg. 1 and Alg. 2. The motivation comes from two observations. First, both *doubleGreedy* and

¹It has been proved that no approximation algorithm can provide better than $\frac{1}{2}$ approximation with polynomial times of oracle calls [35].

Algorithm 1: doubleGreedyWithOrder($f(\cdot), \mathcal{S}$)

```
1 Let  $X_0 \leftarrow \emptyset, Y_0 \leftarrow \mathcal{S}, U \leftarrow \mathcal{S}$ .
2 for  $i = 1$  to  $|\mathcal{S}|$  do
3    $u_i \leftarrow \arg \max_{u \in U} \Delta_f(u \mid X_{i-1})$ .
4    $U \leftarrow U \setminus \{u_i\}$ .
5   Let  $a_i \leftarrow \max\{f(X_{i-1} \cup \{u_i\}) - f(X_{i-1}), 0\}$ .
6   Let  $b_i \leftarrow \max\{f(Y_{i-1} \setminus \{u_i\}) - f(Y_{i-1}), 0\}$ .
7    $p \leftarrow$  random variable from  $[0, 1]$ .
8   if  $p > a_i / (a_i + b_i)$  then
9      $X_i \leftarrow X_{i-1} \cup \{u_i\}, Y_i \leftarrow Y_{i-1}$ .
10  else
11     $X_i \leftarrow X_{i-1}, Y_i \leftarrow Y_{i-1} \setminus \{u_i\}$ .
12 return  $\mathcal{S}^* \leftarrow X_n$ .
13 *If  $a_i = b_i = 0$ , we assume  $a_i / (a_i + b_i) = 1$ .
```

Algorithm 2: deterministicUSMWithOrder($f(\cdot), \mathcal{S}$)

```
1 Initialize a distribution  $\mathcal{D}_0 = \{(1, (\emptyset, \mathcal{S}))\}$ ,  $U \leftarrow \mathcal{S}$ .
2 for  $i = 1$  to  $|\mathcal{S}|$  do
3    $(X^{\max}, Y^{\max}) \leftarrow \arg \max_{(X, Y) \in \text{supp}(\mathcal{D}_{i-1})} P[(X, Y)]$ .
4    $u_i \leftarrow \arg \max_{u \in U} \Delta_f(u \mid X^{\max})$ .
5    $U \leftarrow U \setminus \{u_i\}$ .
6    $\forall (X, Y) \in \text{supp}(\mathcal{D}_{i-1})$ , let
7      $a_i(X) = f(X \cup \{u_i\}) - f(X)$ ,
8      $b_i(Y) = f(Y \setminus \{u_i\}) - f(Y)$ .
9   Find an extreme point solution of the following linear
10  program problem:
11      $\mathbb{E}_{\mathcal{D}_{i-1}}[z(X, Y)a_i(X) + \omega(X, Y)b_i(Y)] \geq 2 \cdot \mathbb{E}_{\mathcal{D}_{i-1}}[z(X, Y)b_i(Y)]$ 
12      $\mathbb{E}_{\mathcal{D}_{i-1}}[z(X, Y)a_i(X) + \omega(X, Y)b_i(Y)] \geq 2 \cdot \mathbb{E}_{\mathcal{D}_{i-1}}[\omega(X, Y)a_i(Y)]$ 
13      $z(X, Y) + \omega(X, Y) = 1, z(X, Y), \omega(X, Y) \geq 0, \forall (X, Y) \in \text{supp}(\mathcal{D}_{i-1})$ 
14 8    $\forall (X, Y) \in \text{supp}(\mathcal{D}_{i-1})$ , add following to a new
15  distribution  $\mathcal{D}_i$ :
16      $\{(z(X, Y) \cdot P[(X, Y)], (X + u_i, Y)) \mid z(X, Y) > 0\}$ 
17      $\cup \{(\omega(X, Y) \cdot P[(X, Y)], (X, Y - u_i)) \mid \omega(X, Y) > 0\}$ 
18 9 return  $\mathcal{S}^* \leftarrow \arg \max_{(X, Y) \in \text{supp}(\mathcal{D}_n)} \{f(X)\}$ .
19 10 * $\text{supp}(\mathcal{D})$  represents the support of the distribution  $\mathcal{D}$ .
```

deterministicUSM algorithms have no requirements on the ordering of elements in the ground set. Second, we find that the greedy-based algorithm (introduced in Sec. V-C) usually provides better results compared with these approximation algorithms, although it has no optimality guarantees. Therefore, we introduce ordering heuristics to facilitate the advantage of the greedy algorithm while preserving the optimality guarantees. Specifically, for the doubleGreedy algorithm, the next loop edge is selected as the one that has the maximum contribution given existing X_{i-1} (lines 3-4 of Alg. 1). And for the deterministicUSM algorithm, the next loop edge is selected as the best loop edge given X^{\max} , where (X^{\max}, Y^{\max}) is the pair of set that has highest probability in previous distribution \mathcal{D}_{i-1} (lines 3-5 of Alg. 2).

Lazy-check strategy: The ordering heuristics require $\mathcal{O}(|\mathcal{S}|)$ oracle queries in each iteration, resulting in total oracle queries of order $\mathcal{O}(|\mathcal{S}|^2)$. However, they can be significantly reduced by the lazy-check strategy, as shown in Tab. I. Specifically, we can maintain a heap to store the unvisited elements in U , and only update the value of the top element of the heap to find the best candidate loop edge in each iteration of algorithms.

Proposition 2: Alg. 1 and Alg. 2 provide $\frac{1}{2}$ -optimality

guarantee for Problem 1.

The proof of Prop. 2 follows the proofs in [33] and [34], and that adding ordering heuristics does not affect the proof.

Proposition 3: Alg. 1 and Alg. 2 require $\mathcal{O}(|\mathcal{S}|^2)$ oracle queries, and the double greedy algorithm without ordering heuristics requires $\mathcal{O}(|\mathcal{S}|)$ oracle queries.

C. Simple Greedy-based Algorithm

Here we also propose a simple greedy algorithm, which, however, has no optimality guarantees. Specifically, the greedy algorithm selects the loop edge that contributes most to the objective function from \mathcal{S} in each iteration and terminates until no candidate loop edge can further improve the objective value. The lazy-check strategy can also be used to improve its time efficiency, as compared in Tab. I.

VI. EXPERIMENTS

This section simulates various 2D graph environments of different sizes for multi-robot exploration. We use OR-Tools [29] as the VRP solver and the MILP solver in Sec. IV-E. The time limit for VRP pathfinding is set as 20 seconds. The linear program (LP) problem in Alg. 2 is solved by *pulp*², with an objective function defined as minimizing $0.5 \cdot \sum z(X, Y) + 0.6 \cdot \sum \omega(X, Y)$. By default, we take $\lambda = 0.3$ in Eq. (6) to get α in Problem 1. We compare the performance of five algorithms, *i.e.*, doubleGreedy (dGre), doubleGreedy+Ordering (dGre+order), deterministicUSM (dUSM), deterministicUSM+Ordering (dUSM+order), and simpleGreedy (sGre). All algorithms are implemented in Python 3 and tested on a desktop with an i9-13900 CPU and 32 GB of RAM.

A. Random Generation of Graph Experiments

The graph environments are randomly derived from grid-like structures of different sizes, *i.e.*, $60m \times 60m$, $80m \times 80m$, $100m \times 100m$, $120m \times 120m$, with a grid step as ten meters. An example graph covering a $100m \times 100m$ area is shown in Fig. 1. Each vertex in a grid graph is only connected to its adjacent vertices. Then 10% vertices (and their outgoing edges) and additional 3% edges are randomly removed to create diverse topologies. Finally, Gaussian noise of $\mathcal{N}(0, 2m)$ is added to the xy coordinates of vertices in the graph. The covariance matrix Σ_{ij} for each edge in $\mathcal{G}_{\mathcal{R}}^{\text{pose}}$ and the set \mathcal{S} is set as $\text{diag}\{0.1m, 0.1m, 0.001\text{rad}\}$. Fifty random graphs are independently generated for each environment size. By default, three robots starting from the same vertex are deployed in the graph exploration tasks.

B. Relationship Verification of FIM and Graph Laplacian

We first verify the relation between the log determinant of full FIM in multi-robot pose graph optimization and the corresponding weighted pose graph Laplacian matrix, as shown in Fig. 3(a). Each point in Fig. 3(a) corresponds to a multi-robot pose graph with random sets of loop edges added to it. Similar to the results in [21], the two metrics have a positive correlation with each other. Moreover, the graph

²<https://github.com/coin-or/pulp>

TABLE I
RUNNING TIME COMPARISON

Env (m^2)	sGre	sGre(l-c)	dGre [33]	dGre+order	dGre+order(l-c)	dUSM [34]	dUSM+order	dUSM+order(l-c)
60×60	0.050	0.017	0.061	0.170	0.054	1.389	1.373	1.243
80×80	0.218	0.050	0.133	0.692	0.183	6.164	6.762	6.023
100×100	0.922	0.139	0.296	2.428	0.489	18.467	19.816	16.923
120×120	4.389	0.483	0.948	10.313	1.733	77.212	72.687	63.868

Note: The unit for all data in the table is seconds; each item is the averaged result over fifty experiments; l-c stands for lazy-check.

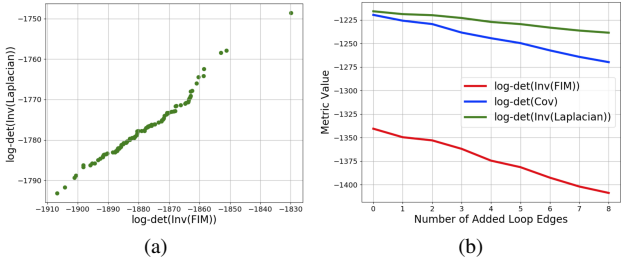


Fig. 3. (a) The relationship between $\log \det(\mathbf{L}_\gamma^{-1})$ and $\log \det(\mathbf{I}^{-1})$ evaluated on a set of pose graphs derived from a $120m \times 120m$ graph environment; (b) The pose estimation uncertainty decreases as more loop edges are added into the multi-robot pose graph.

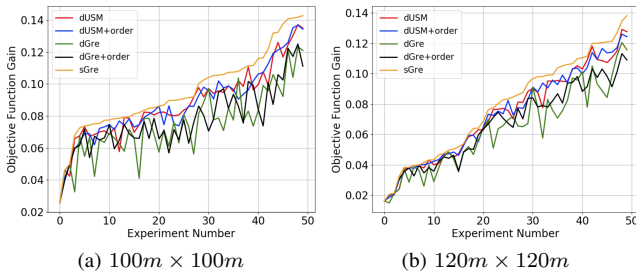


Fig. 4. The objective gain of Problem 1 with the five algorithms in 50 independent experiments. Results for $60m \times 60m$ and $80m \times 80m$ are not shown due to space constraints. Note the results are sorted according to the objective value of the sGre algorithm for better visualization.

topology metric $\log \det(\mathbf{L})$ preserves action consistency with the original FIM metric when evaluating candidate loop edges. Therefore, it is reasonable to use the graph topology metric in Problem 1 for pose graph uncertainty evaluation, which brings lower computational complexity than the original FIM metric. Fig. 3(b) shows the changing trend of the full covariance matrix (obtained from GTSAM³), full FIM, and the reduced weighted Laplacian matrix as more loop edges are added into $\mathcal{G}_R^{\text{pose}}$. Without accounting for the distance cost, the three metrics decrease monotonically, indicating that the pose uncertainty in SLAM reduces as the connectivity of the multi-robot pose graph improves, and thereby the graph topology metric in Problem 1 encourages adding loop edges into the robots' paths.

C. Performance Comparison in Loop Edge Selection

Fig. 4 shows the performance of the five algorithms in loop edge selection problems over various environments. The averaged running time of the algorithms is shown in Tab. I. Generally, the sGre algorithm provides the best results compared with others, although it has no performance guarantee. For the four approximation algorithms that provide $\frac{1}{2}$

³<https://github.com/borglab/gtsam>

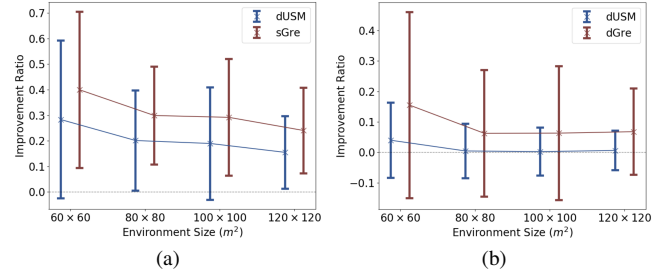


Fig. 5. (a) The objective improvement ratio of the dUSM and sGre algorithms w.r.t. the dGre algorithm; (b) The objective improvement ratio after adding the ordering heuristics to dGre and dUSM algorithms.

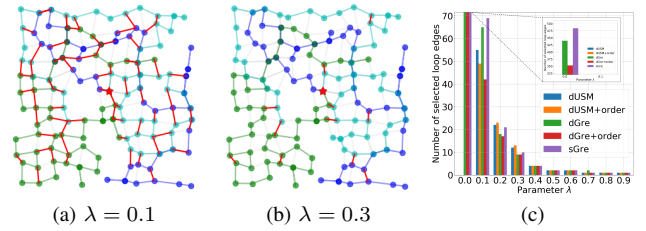


Fig. 6. The loop edge selection problem defined over a $120m \times 120m$ graph environment with 11303 candidate loop edges. Robots' paths are painted in different colors. (a) and (b) show the final selected loop edges (red) by the sGre algorithm with different λ in Eq. (6); (c) shows the comparison of the number of selected loop edges with different λ . Note the results of dUSM and dUSM+order are missing when $\lambda = 0$ because the two algorithms cannot output the results within an hour.

optimality guarantees, the dUSM algorithm generally gets better results than the dGre algorithm. However, it spends significantly more time than the dGre algorithm as in Tab. I, because it solves a linear program in each iteration, which dominates the computational time. The dGre algorithm usually gets the worst results, as shown in Fig. 5(a), that the objective value of sGre and dUSM algorithms are 31% and 21% better than the dGre algorithm respectively. However, it runs faster than the dUSM algorithm by an order of magnitude while still providing optimality guarantees. On average, adding ordering heuristics to the dGre algorithm can improve its performance by 9%, while no discernible improvement is observed for the dUSM algorithm, as shown in Fig. 5(b). The ordering heuristics also introduces extra time complexity, as in Tab. I. However, the extra time expense can be significantly reduced by applying the lazy-check strategy introduced in Sec. V-B, which also makes the sGre algorithm the fastest among all the compared algorithms.

Additionally, we also evaluate the effect of the parameter λ in Eq. (6) on the number of finally selected loop edges in Problem 1, as shown in Fig. 6. As λ increases from 0 to 1, the number of selected loop edges decreases significantly, which controls the frequency of active loop-closing actions

in the final paths, and also balances the distance cost during exploration, as we analyzed in Sec. IV-D.

VII. CONCLUSION AND FUTURE WORK

This paper investigates a multi-robot active graph exploration problem considering both exploration efficiency and pose graph reliability in multi-robot SLAM. A two-stage strategy is proposed to find quick coverage paths with informative and distance-efficient loop edges. Moreover, approximation algorithms in submodular optimization are employed to provide optimality guarantees for the loop edge selection problem. We validate the effectiveness of the proposed methods with simulated graph exploration experiments, and benchmark the performance of approximation algorithms and the greedy algorithm.

The proposed method is limited to application scenarios where prior topological-metric information about the environment is available, *i.e.*, a city-scale mapping task with a prior roadmap, or an indoor exploration task with a brief floorplan. The proposed method can be applied as a high-level path planner in these tasks. Future work is to incorporate the proposed path planner into a multi-robot SLAM system for collaborative exploration and pose estimation.

REFERENCES

- [1] Y. Tian, K. Liu, K. Ok, L. Tran, D. Allen, N. Roy, and J. P. How, "Search and rescue under the forest canopy using multiple uavs," *The International Journal of Robotics Research*, vol. 39, no. 10-11, pp. 1201–1221, 2020.
- [2] R. Bai, R. Zheng, Y. Xu, M. Liu, and S. Zhang, "Hierarchical multi-robot strategies synthesis and optimization under individual and collaborative temporal logic specifications," *Robotics and Autonomous Systems*, vol. 153, p. 104085, 2022.
- [3] X. Xu, M. Cao, S. Yuan, T. H. Nguyen, T.-M. Nguyen, and L. Xie, "A cost-effective cooperative exploration and inspection strategy for heterogeneous aerial system," in *2024 IEEE 18th International Conference on Control & Automation (ICCA)*, pp. 673–678, 2024.
- [4] Y. Tian, Y. Chang, F. Herrera Arias, C. Nieto-Granda, J. P. How, and L. Carlone, "Kimera-Multi: Robust, distributed, dense metric-semantic SLAM for multi-robot systems," *IEEE Transactions on Robotics*, vol. 38, no. 4, pp. 2022–2038, 2022.
- [5] H. Guo, J. Zhu, and Y. Chen, "E-loam: Lidar odometry and mapping with expanded local structural information," *IEEE Transactions on Intelligent Vehicles*, vol. 8, no. 2, pp. 1911–1921, 2023.
- [6] S. Yuan, H. Wang, and L. Xie, "Survey on localization systems and algorithms for unmanned systems," *Unmanned Systems*, vol. 9, no. 02, pp. 129–163, 2021.
- [7] P. Lajoie, B. Ramtoula, F. Wu, and G. Beltrame, "Towards collaborative simultaneous localization and mapping: a survey of the current research landscape," *CoRR*, vol. abs/2108.08325, 2021.
- [8] G. Grisetti, R. Kümmerle, C. Stachniss, and W. Burgard, "A tutorial on graph-based SLAM," *IEEE Intelligent Transportation Systems Magazine*, vol. 2, no. 4, pp. 31–43, 2010.
- [9] Z. Zhang, J. Yu, J. Tang, Y. Xu, and Y. Wang, "MR-TopoMap: Multi-robot exploration based on topological map in communication restricted environment," *IEEE Robotics and Automation Letters*, vol. 7, no. 4, pp. 10794–10801, 2022.
- [10] A. Kitanov and V. Indelman, "Topological belief space planning for active SLAM with pairwise Gaussian potentials and performance guarantees," *The International Journal of Robotics Research*, p. 02783649231204898, 2023.
- [11] J. Yan, X. Lin, Z. Ren, S. Zhao, J. Yu, C. Cao, P. Yin, J. Zhang, and S. Scherer, "Mui-tare: Cooperative multi-agent exploration with unknown initial position," *IEEE Robotics and Automation Letters*, vol. 8, no. 7, pp. 4299–4306, 2023.
- [12] S. Zhong, Y. Qi, Z. Chen, J. Wu, H. Chen, and M. Liu, "Dcl-slam: A distributed collaborative lidar slam framework for a robotic swarm," *IEEE Sensors Journal*, vol. 24, no. 4, pp. 4786–4797, 2024.
- [13] J. Vallvé and J. Andrade-Cetto, "Active pose SLAM with RRT," in *2015 IEEE International Conference on Robotics and Automation (ICRA)*, pp. 2167–2173, 2015.
- [14] N. Atanasov, J. Le Ny, K. Daniilidis, and G. J. Pappas, "Decentralized active information acquisition: Theory and application to multi-robot SLAM," in *2015 IEEE International Conference on Robotics and Automation (ICRA)*, pp. 4775–4782, 2015.
- [15] Y. Kantaros, B. Schlotfeldt, N. Atanasov, and G. J. Pappas, "Sampling-based planning for non-myopic multi-robot information gathering," *Autonomous Robots*, vol. 45, no. 7, pp. 1029–1046, 2021.
- [16] X. Cai, B. Schlotfeldt, K. Khosoussi, N. Atanasov, G. J. Pappas, and J. P. How, "Non-monotone energy-aware information gathering for heterogeneous robot teams," in *2021 IEEE International Conference on Robotics and Automation (ICRA)*, pp. 8859–8865, 2021.
- [17] Y. Chen, L. Zhao, K. M. B. Lee, C. Yoo, S. Huang, and R. Fitch, "Broadcast your weaknesses: cooperative active pose-graph SLAM for multiple robots," *IEEE Robotics and Automation Letters*, vol. 5, no. 2, pp. 2200–2207, 2020.
- [18] J. A. Placed and J. A. Castellanos, "Fast autonomous robotic exploration using the underlying graph structure," in *2021 IEEE/RSJ International Conference on Intelligent Robots and Systems (IROS)*, pp. 6672–6679, 2021.
- [19] K. Khosoussi, M. Giamou, G. S. Sukhatme, S. Huang, G. Dissanayake, and J. P. How, "Reliable graphs for SLAM," *The International Journal of Robotics Research*, vol. 38, no. 2-3, pp. 260–298, 2019.
- [20] Y. Chen, S. Huang, L. Zhao, and G. Dissanayake, "Cramér–Rao bounds and optimal design metrics for pose-graph SLAM," *IEEE Transactions on Robotics*, vol. 37, no. 2, pp. 627–641, 2021.
- [21] J. A. Placed and J. A. Castellanos, "A general relationship between optimality criteria and connectivity indices for active graph-SLAM," *IEEE Robotics and Automation Letters*, vol. 8, no. 2, pp. 816–823, 2023.
- [22] R. Bai, H. Guo, W.-Y. Yau, and L. Xie, "Graph-based slam-aware exploration with prior topo-metric information," *IEEE Robotics and Automation Letters*, pp. 1–8, 2024.
- [23] K. Khosoussi *et al.*, "Novel insights into the impact of graph structure on SLAM," in *2014 IEEE/RSJ International Conference on Intelligent Robots and Systems (IROS)*, pp. 2707–2714, 2014.
- [24] H. Carrillo *et al.*, "On the comparison of uncertainty criteria for active SLAM," in *2012 IEEE International Conference on Robotics and Automation (ICRA)*, pp. 2080–2087, 2012.
- [25] A. Pázman, "Foundations of optimum experimental design," 1986.
- [26] S. Obwald *et al.*, "Speeding-up robot exploration by exploiting background information," *IEEE Robotics and Automation Letters (RA-L)*, vol. 1, no. 2, pp. 716–723, 2016.
- [27] J. Kim and H. I. Son, "A voronoi diagram-based workspace partition for weak cooperation of multi-robot system in orchard," *IEEE Access*, vol. 8, pp. 20676–20686, 2020.
- [28] P. Toth and D. Vigo, *The vehicle routing problem*. Society for Industrial and Applied Mathematics, 2002.
- [29] L. Perron and V. Furnon, "Or-tools."
- [30] G. Grisetti, R. Kümmerle, C. Stachniss, U. Frese, and C. Hertzberg, "Hierarchical optimization on manifolds for online 2d and 3d mapping," in *2010 IEEE International Conference on Robotics and Automation (ICRA)*, pp. 273–278, 2010.
- [31] Y. Chen, S. Huang, R. Fitch, L. Zhao, H. Yu, and D. Yang, "On-line 3D active pose-graph SLAM based on key poses using graph topology and sub-maps," in *2019 International Conference on Robotics and Automation (ICRA)*, pp. 169–175, 2019.
- [32] G. Kirchhoff, "On the solution of the equations obtained from the investigation of the linear distribution of galvanic currents," *IRE Transactions on Circuit Theory*, vol. 5, no. 1, pp. 4–7, 1958.
- [33] N. Buchbinder, M. Feldman, J. Naor, and R. Schwartz, "A tight linear time (1/2)-approximation for unconstrained submodular maximization," in *2012 IEEE 53rd Annual Symposium on Foundations of Computer Science*, pp. 649–658, 2012.
- [34] N. Buchbinder and M. Feldman, "Deterministic algorithms for submodular maximization problems," *ACM Transactions on Algorithms (TALG)*, vol. 14, no. 3, pp. 1–20, 2018.
- [35] U. Feige, V. S. Mirrokni, and J. Vondrák, "Maximizing non-monotone submodular functions," *SIAM Journal on Computing*, vol. 40, no. 4, pp. 1133–1153, 2011.